Supplementary Information

A MEK-independent role for CRAF in mitosis and tumor progression.

Ainhoa Mielgo, Laetitia Seguin, Miller Huang, Maria Fernanda Camargo, Sudarshan Anand, Aleksandra Franovic, Sara M. Weis, Sunil J. Advani, Eric Murphy and David A. Cheresh

Supplementary Figure 1. Allosteric inhibition of RAF arrests cells at pro-metaphase in a way that is MEK-independent but requires CRAF phosphorylation on serine 338.

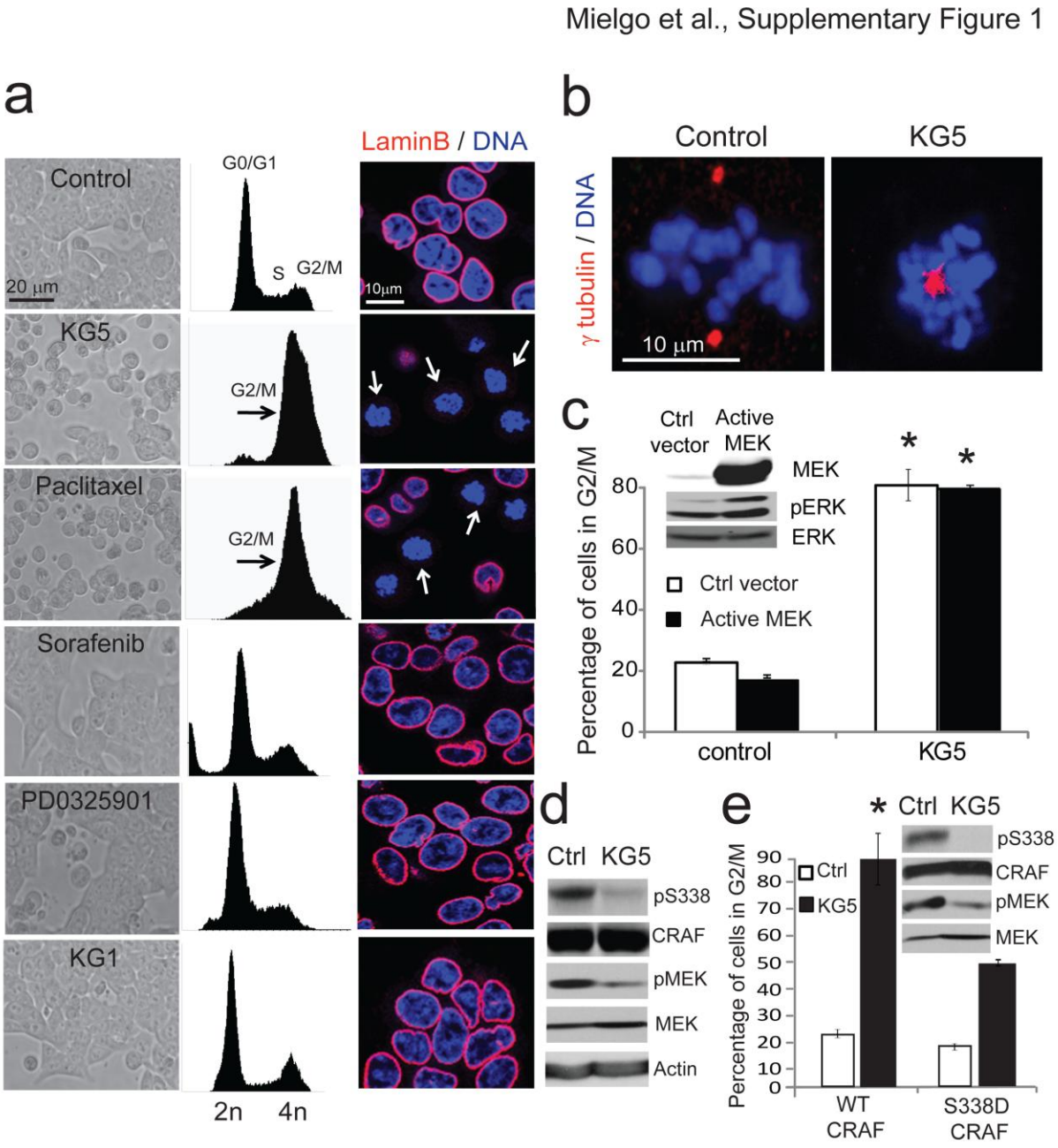

(**a**) Bright field images (scale bar, 20 μm), cell cycle analysis and confocal microscopy images (scale bar, 10 μm, lamin B in red and DNA in blue) of XPA-1 cells treated for 20 hours with the allosteric RAF inhibitor KG5, the ATP-competitive inhibitor Sorafenib, the MEK inhibitor PD0325901, the control compound KG1 at 5 μM or paclitaxel at 200 nM. Cells were harvested after 20 hours and the cell cycle stage was determined by flow cytometry and confocal microscopy. White arrows indicate cells arrested at pro-metaphase. Scale bars, 10 μm. (**b**) Representative confocal microscopy images of untreated XPA-1 tumor cells undergoing mitosis (left image) and XPA-1 cell arrested with KG5 at pro-metaphase (right image). Cells were stained with α tubulin in red and DNA in blue. Scale bar, 10 μm. (**c**) XPA-1 cells transfected with a vector control or active MEK were treated with 1 μM KG5 for 20 hours or left untreated and the G2/M population was quantified by flow cytometry. Error bars represent s.d. (n=3); * two tailed p value = 0.00063 using a Mann Whitney U test. (**d**) Immunoblot analysis of XPA-1 cells untreated or treated with 1 μM KG5 for 18 hours. Data are representative of four independent experiments. (**e**) HCT-116 cells stably expressing WT or the phospho-mimetic S338D CRAF construct were treated with 1 μM KG5 for 18 hours and cells arrested in G2/M were quantified by flow cytometry. Error bars represent s.d. (n=3); * two tailed p value = 0.010 using a Mann Whitney U test. Inset, Immunoblot analysis of HCT-116 cells untreated or treated with 1 μM KG5 for 18 hours.

Supplementary Figure 2. Allosteric inhibition of RAF with KG5, unlike ATP-competitive RAF inhibitors, induces a G2/M arrest followed by cell death.

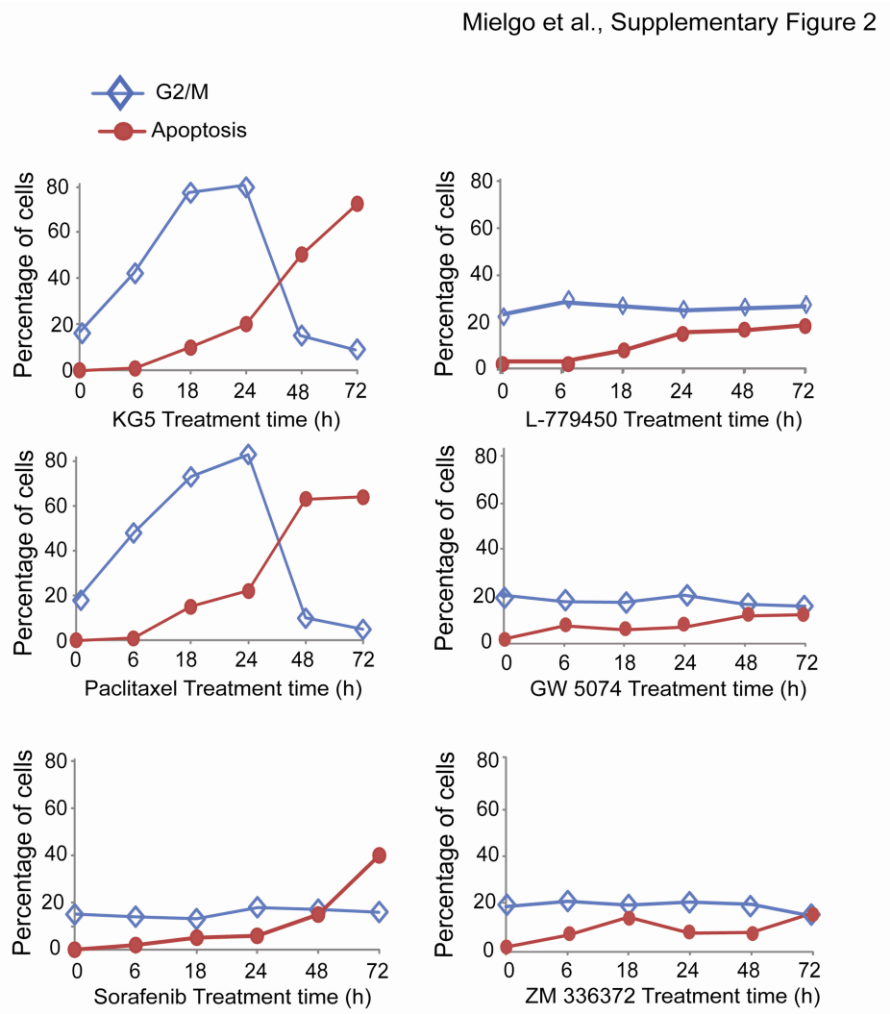

Cell cycle analysis of XPA-1 cells treated with the allosteric RAF inhibitor KG5, the microtubule stabilizer paclitaxel, or the ATP-competitive RAF inhibitors sorafenib, L-779450, GW 5074, and ZM-336372. Cells were harvested after 6, 18, 24, 48 and 72

hours and the percentages of cells in G2/M and SubG1 were determined by flow cytometry. Data are representative of three independent experiments.

Supplementary Figure 3. Allosteric inhibition of RAF arrests proliferating cells at pro-metaphase.

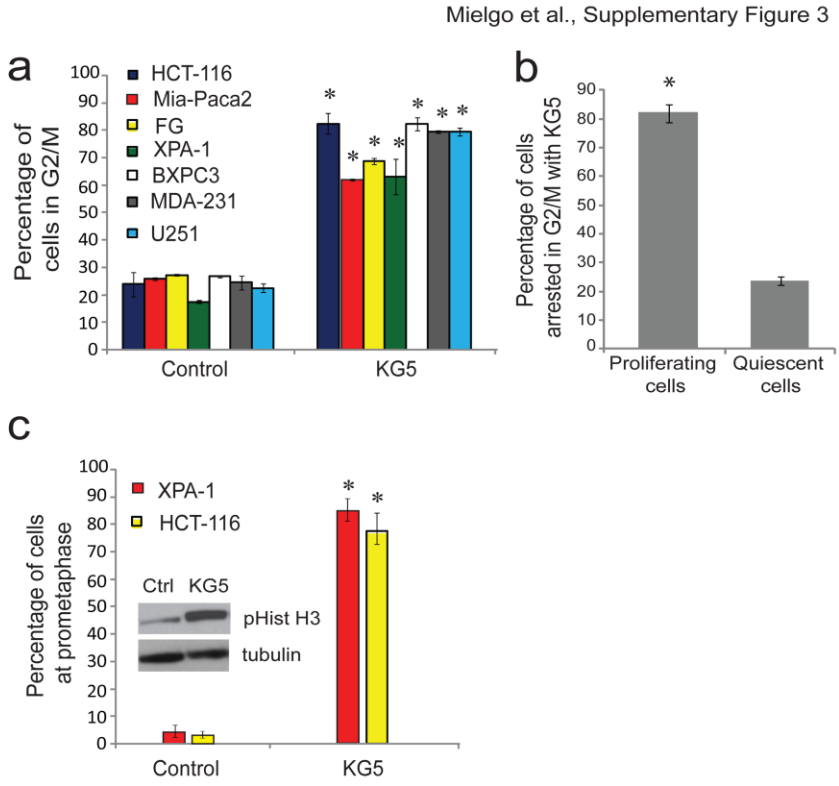

(**a**) Cell cycle analysis and G2/M quantification of human colon (HCT-116), pancreatic (Mia-Paca2, FG, XPA-1, BXPC3), breast (MDA-MB-231) and brain (U251) cancer cell lines untreated or treated for 20 hours with 5 μM of KG5. Error bars represent s.d. (n=4); * two tailed p value = 0.0023 using Mann Whitney U test. (**b**) HCT-116 cells were cultured under low (30%) or high (90%) confluency and treated with 1 μM KG5 for 20 hours. Quantification of cells arrested in G2/M was performed by flow cytometry. Error

bars represent s.d. (n=3); * two tailed p value = 0.0021 using Mann Whitney U test. (**c**) HCT-116 and XPA-1 cells were treated for 20 hours with 1 μM of KG5, stained for α Tubulin/DNA, and cells arrested in pro-metaphase were quantified by confocal microscopy. Error bars represent s.d. (n=3); * two tailed p value = 0.0008 using Mann Whitney U test. Lysates from the same cells were also analyzed by immunoblotting for the expression of the mitotic marker phospho-Histone H3 (inset). Data are representative of three independent experiments.

Supplementary Figure 4. Phospho-S338 CRAF is highly expressed in tumors and can be blocked by an allosteric RAF inhibitor.

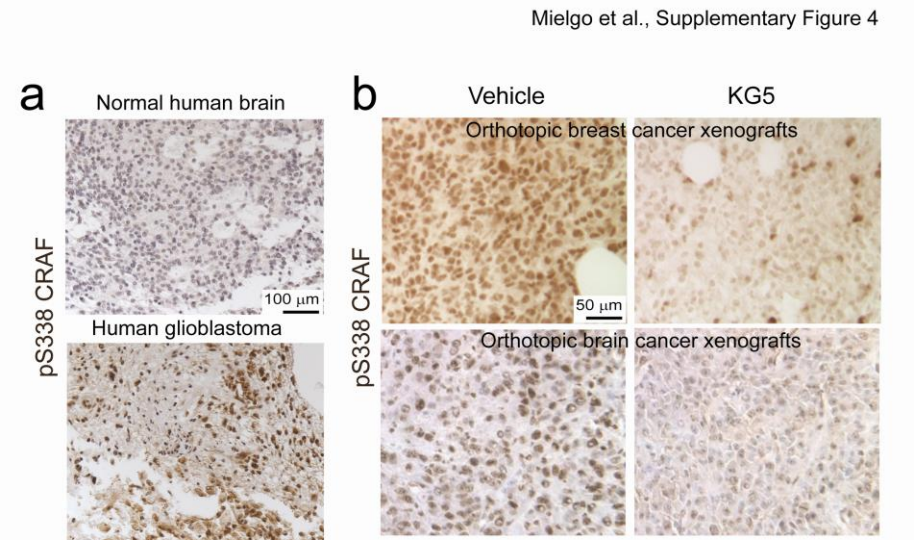

(**a**) Immunohistochemical staining of phospho- S338 CRAF in normal human brain and human glioblastoma tissues. Scale bar, 100 μm. (**b**) Immunohistochemical staining of phospho- S338 CRAF in orthotopic brain tumor xenografts untreated or treated systemically with KG5 (50mg Kg^{-1}) for 3 days. Scale bar, 50 μm.

Supplementary Figure 5. Phospho-S338 CRAF promotes mitosis.

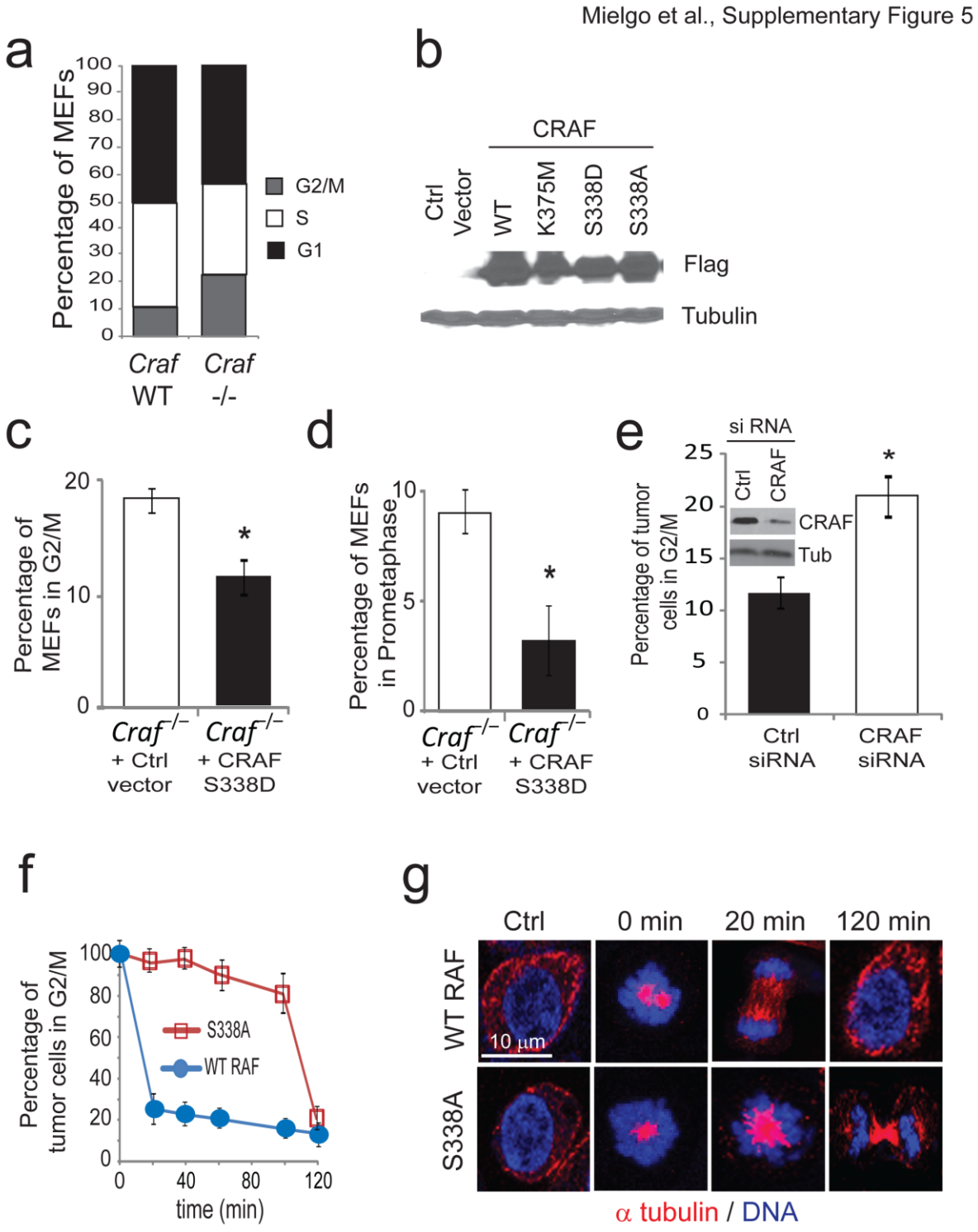

(**a**) Quantification of WT and *Craf*$^{-/-}$ cells in the G1, S and G2/M phases of the cell cycle. Data are representative of three independent experiments. (**b**) Immunoblot analysis of *Craf*$^{-/-}$ MEFs transfected with WT, kinase dead (K375M), phospho-mimetic (S338D) and non-phosphorylatable (S338A) FLAG tagged CRAF constructs. (**c**) Cell cycle analysis of *Craf*$^{-/-}$ MEFs transfected with vector control or S338D CRAF was performed. Cells in G2/M were quantified by flow cytometry. Error bars represent s.d. (n=3); * two tailed p value = 0.0067 using a Mann Whitney U test. (**d**) Cells at pro-metaphase were quantified using confocal microscopy. Error bars represent s.d. (n=3); * two tailed p value = 0.0048 using a Mann Whitney U test. (**e**) HCT-116 cells were transfected with control or CRAF siRNAs and cells in G2/M were quantified by flow cytometry. Error bars represent s.d. (n=3); * two tailed p value = 0.0062 using a Mann Whitney U test. Lysates of these cells were analyzed for CRAF expression by immunoblotting (inset). (**f**) XPA-1 cells ectopically expressing either WT RAF or S338A mutant CRAF were arrested in pro-metaphase as described in Methods, and subsequently allowed to progress through mitosis. Quantification of cells in G2/M was performed by flow cytometry. Error bars represent s.d. (n=3). (**g**) Confocal microscopy images of cells progressing through mitosis at 0, 20, 100 and 120 minutes after release from pro-metaphase blockade. Cells were stained for α tubulin (in red) and DNA (TOPRO-3 in blue). Scale bar, 10 μm.

Supplementary Figure 6. Phospho-S338 CRAF localizes to centrosomes in G2 phase and spindle poles during tumor cell mitosis.

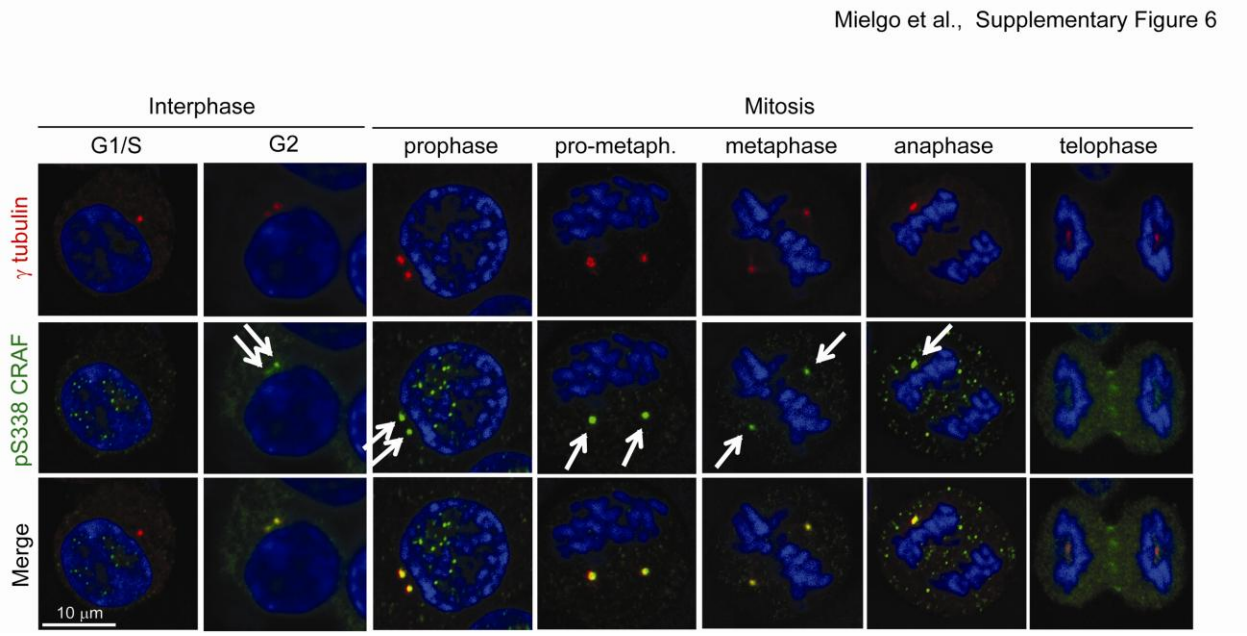

Confocal microscopy images of human HCT-116 cells synchronized at the G1/S boundary by a double thymidine block (as described in Methods) and stained for γ tubulin (in red), phospho-S338 CRAF (in green), and DNA (TOPRO-3 in blue). Scale bar, 10 μm. White arrows indicate localization of phospho-S338 CRAF at the centrosomes in G2 and the mitotic spindle poles from pro-metaphase to anaphase.

Supplementary Figure 7. Phospho-S338 CRAF localizes to mitotic spindle poles in a BRAF-independent manner.

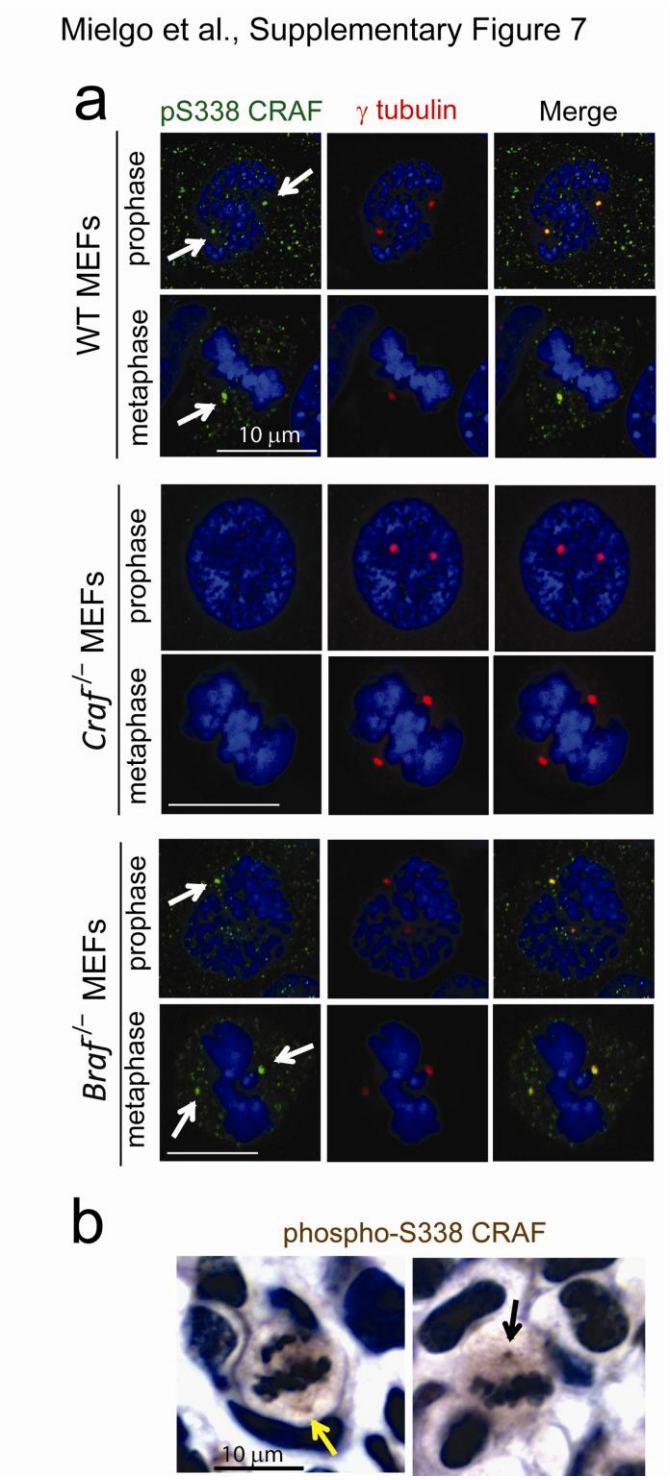

(**a**) Confocal microscopy images of WT, CRAF-/- and BRAF-/- MEFs at prophase and metaphase stained for phospho-S338 CRAF (in green), γ tubulin (in red) and DNA (TOPRO-3 in blue). Scale bar, 10 μm. White arrows indicate localization of phospho-S338 CRAF at the mitotic spindle poles. (**b**) Immunohistochemical staining of phospho-S338 CRAF in tumor biopsies from mouse orthotopic breast tumour xenografts. Scale bar, 10 μm.

Supplementary Figure 8. CRAF interacts with Plk1 and Aurora A and this interaction does not require CRAF kinase activity but requires serine 338 phosphorylation.

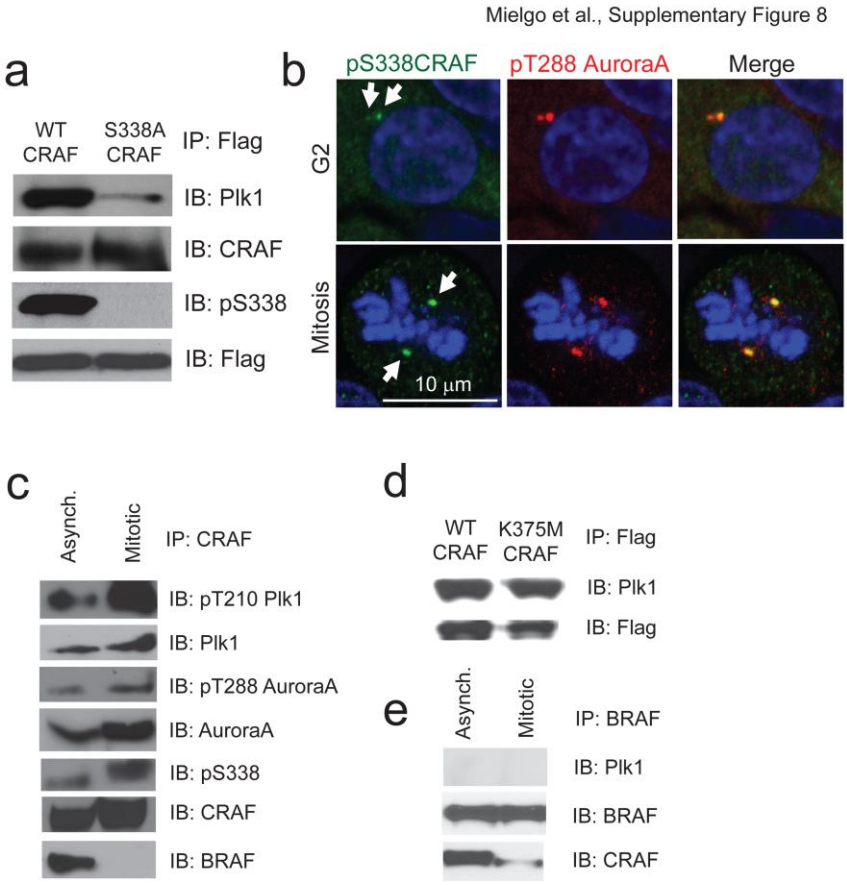

(**a**) Immunoblot analysis of Flag immunoprecipitates from XPA-1 cells expressing Flag-tagged WT or S338A CRAF. Data are representative of three independent experiments. (**b**) Confocal microscopy images of a HCT-116 synchronized in G2 or mitosis (as described in methods) and stained for phospho-S338 CRAF (in green), phospho-T288 Aurora A (in red) and DNA (in blue). White arrows indicate colocalization between phospho-S338 CRAF and phospho-T288 Aurora A. Scale bar, 10 μm. (**c**) Immunoblot analysis of CRAF immunoprecipitates from XPA-1 cells asynchronized or synchronized in mitosis. Data are representative of three independent experiments. (**d**) Immunoblot analysis of Flag immunoprecipitates from XPA-1 cells expressing Flag-tagged WT or kinase dead (K375M) CRAF. Data are representative of three independent experiments.

(**e**) Immunoblot analysis of BRAF immunoprecipitates from HCT-116 cells asynchronized or synchronized in mitosis.

Supplementary Figure 9. CRAF regulates Plk1 activity and localization.

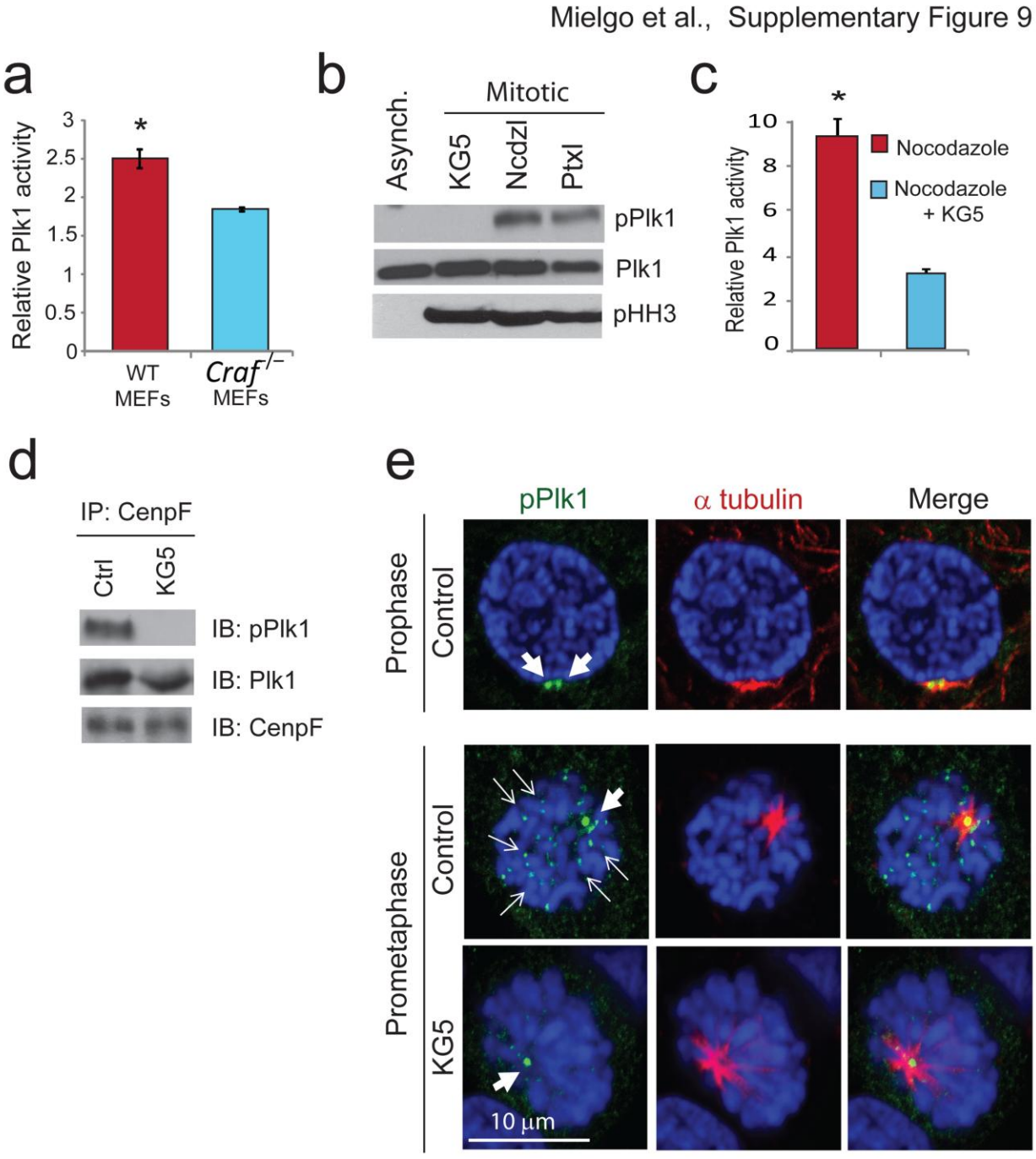

(**a**) Plk1 kinase activity assay performed in WT and CRAF-/- MEFs. Error bars represent s.d. (n=3); * two tailed p value = 0.029 using Mann Whitney U test. (**b**) Immunoblot analysis of XPA-1 cells asynchronous or arrested in mitosis by treatment with KG5, nocodazole or paclitaxel (referred to as Ncdzl and Ptxl respectively). pPlk1 refers to phospho-T210 Plk1 and pHH3 refers to phospho-Histone H3. Data are representative of three independent experiments. (**c**) Plk1 kinase activity assay performed in HCT-116 cells treated with nocodazole or nocodazole and KG5. Error bars represent s.d. (n=2); * two tailed p value = 0.002 using Mann Whitney U test. (**d**) Immunoblot analysis of CenpF immunoprecipitates from HCT-116 cells untreated or treated with KG5. Data are representative of three independent experiments. (**e**) Confocal microscopy images of XPA-1 cell at prophase (upper panel), pro-metaphase control untreated (middle panel) or treated with KG5 (lower panel). Cells were stained for phospho-T210 Plk1 (in green), α tubulin (in red) and DNA (TOPRO-3 in blue). Thick white arrows indicate localization of pPlk1 at the mitotic spindle pole and narrow white arrows indicate localization of pPlk1 at the kinetochores. Scale bar, 10 μm.

Supplementary Figure 10. Allosteric inhibition or depletion of CRAF prevents active Plk1 accumulation at the kinetochores in pro-metaphase.

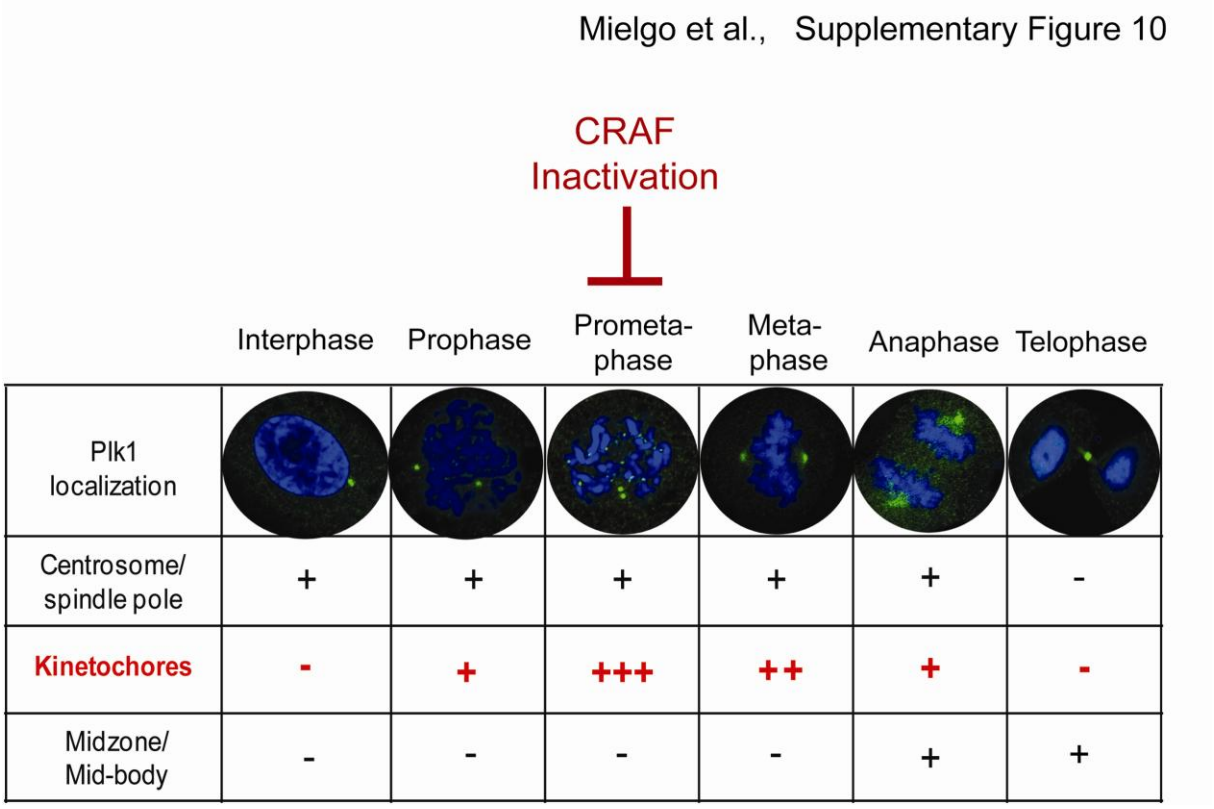

Table indicating Plk1 localization before mitosis and during the different stages of mitosis (from prophase to telophase). Phospho- T210 Plk1 is stained in green and DNA in blue.

Supplementary Figure 11. Kinase dead CRAF and constitutively active T210D Plk1 are both capable of rescuing the *Craf*$^{-/-}$ MEFs phenotype.

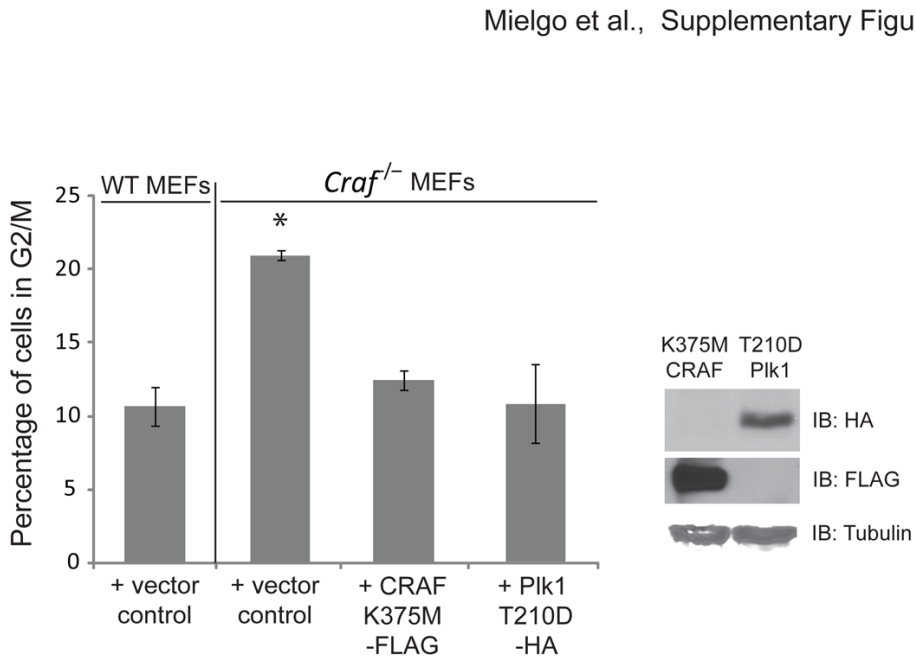

(**a**) *Craf*$^{-/-}$ MEFs were transfected with vector control, kinase dead (K375M) CRAF or a constitutively active T210D Plk1 mutant and the G2/M population was quantified by flow cytometry. Error bars represent s.d. (n=3); * two tailed p value = 0.0055 using a Mann Whitney U test. (**b**) Immunoblot analysis of *Craf*$^{-/-}$ MEFs transfected with kinase dead (K375M) CRAF FLAG tagged or a constitutively active T210D Plk1 HA-tagged mutant.

Supplementary Figure 12. Phospho-mimetic CRAF S338D mutation drives tumor growth in a brain orthotopic model.

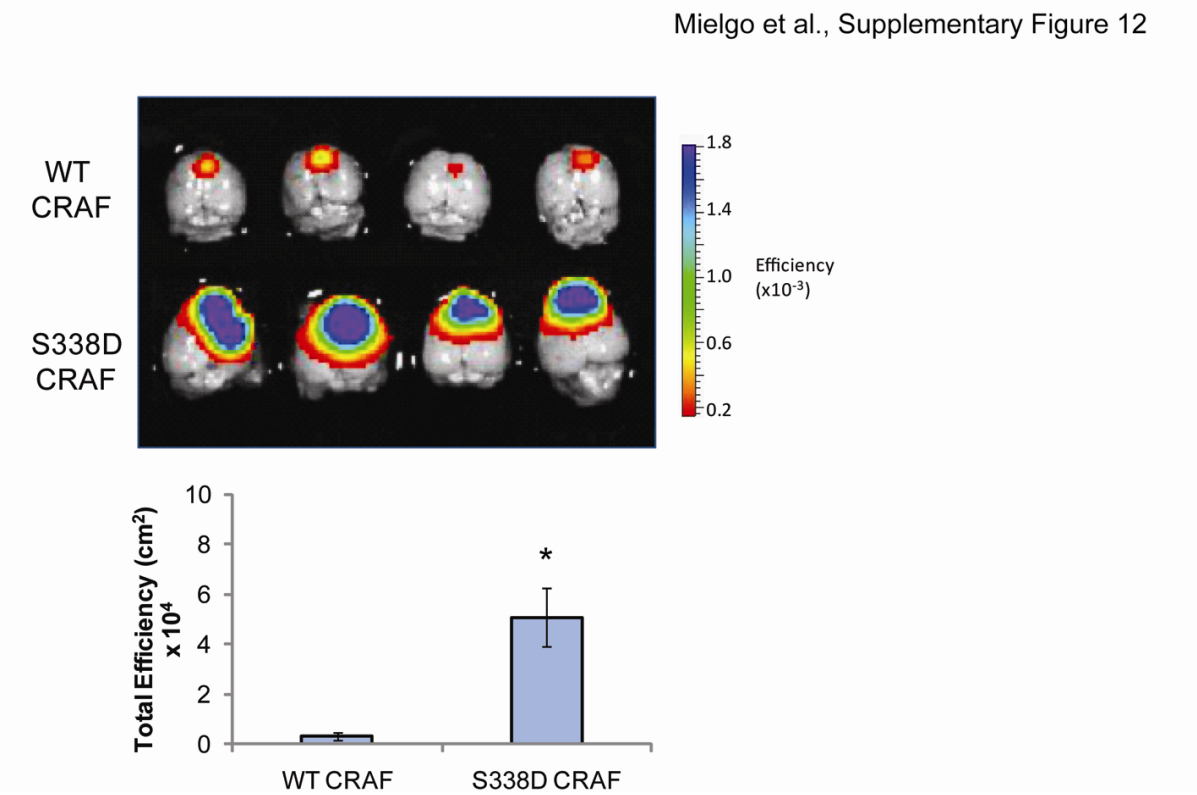

RFP-labeled U-87 human glioblastoma cells expressing WT or S338D CRAF were orthotopically implanted in the brain of immune-compromised nude mice. Fluorescence images were recorded and tumor sizes analyzed using IVIS LivingImage Software. Values are shown as average fluorescence efficiency +/- SD. (n=9); * two tailed p value = 0.003 using Student T test.

Supplementary Figure 13. Phospho-mimetic kinase dead CRAF S338D K375M mutation drives tumor growth.

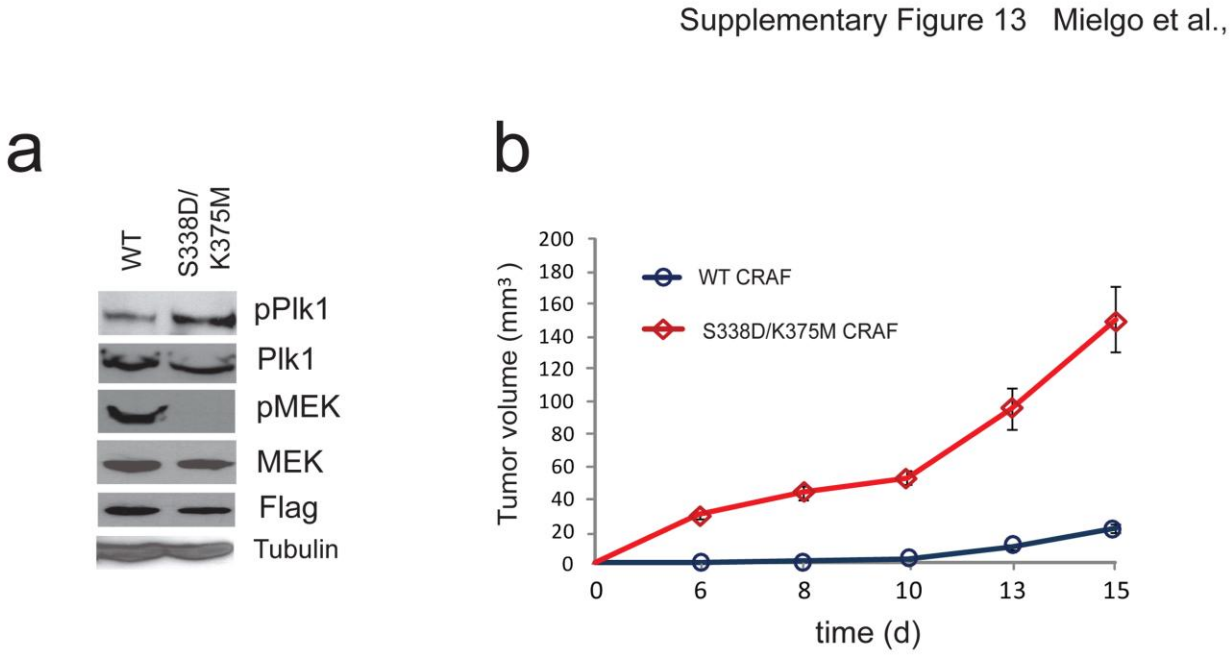

(**a**) Immunoblot analysis of phospho-T210 Plk1, Plk1, phospho-MEK, MEK, Flag and tubulin from U-87 cells expressing WT or S338D/K375M CRAF. Data are representative of five independent experiments. (**b**) U-87 cells expressing WT or S338D/K375M CRAF were injected subcutaneously in the flank of immune-compromised nude mice. Tumor size measurements are shown (n=10).

Supplementary Figure 14. Model depicting the MEK-independent role of CRAF in mitosis and tumor progression.

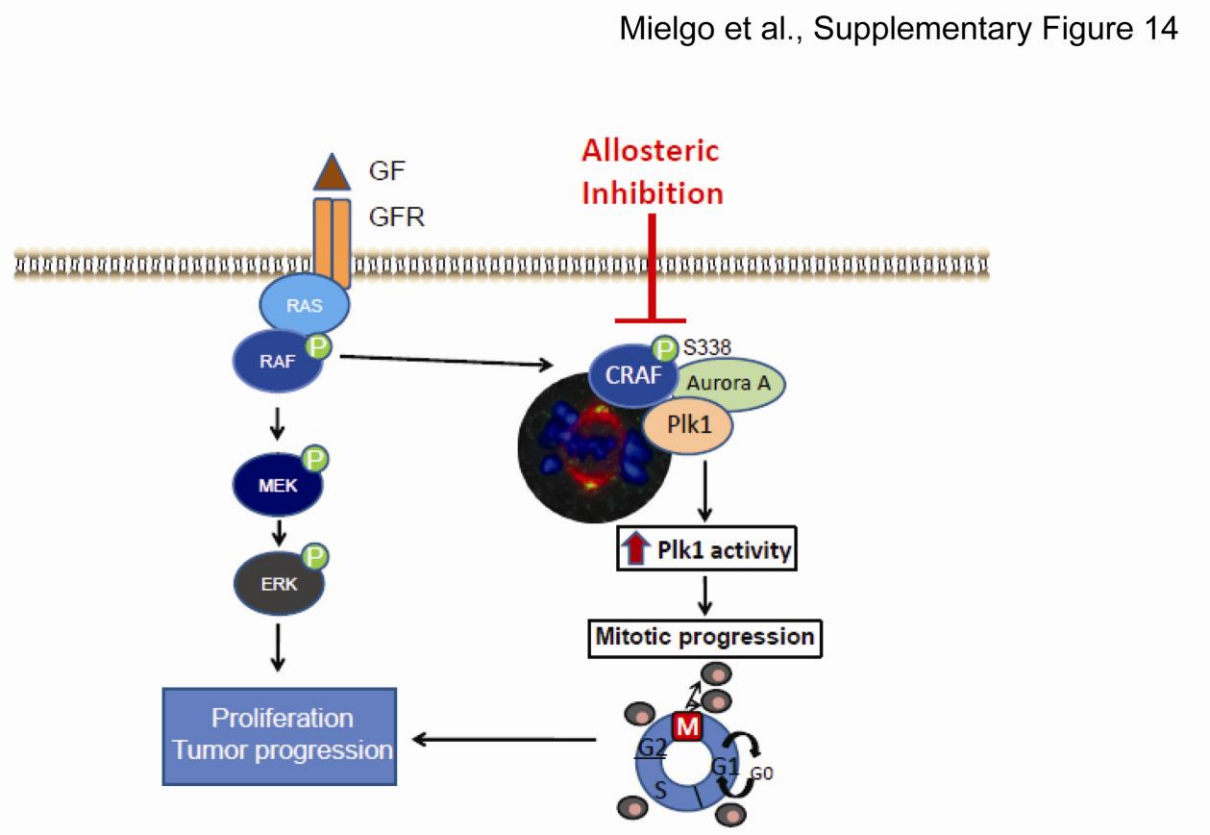

Phospho-S338 CRAF localizes to centrosomes in G2 and mitotic spindle poles in mitosis where it interacts with Plk1 and Aurora A and promotes Plk1 activation, leading to mitosis and tumor progression. Allosteric inhibition of CRAF prevents phosphorylation of CRAF at serine 338, and thereby activation of Plk1, causing cells to arrest at pro-metaphase.

Supplementary Table 1. KG5 effect in 60 NCI cancer cell lines

NCI-60 panel showing the half maximal growth inhibitory concentration of KG5 and the RAS and BRAF status in 60 human cancer cell lines.

Cell line		Mutated RAS	Mutated BRAF	GI50 (nM)
Breast Cancer	BT-549	No	No	708
Breast Cancer	HS 578T	Yes	No	437
Breast Cancer	MCF7	No	No	355
Breast Cancer	MDA-MB-231/ATCC	Yes	Yes	1479
Breast Cancer	MDA-MB-468	No	No	191
Breast Cancer	T-47D	Yes	No	347
CNS Cancer	SF-268	No	No	912
CNS Cancer	SF-295	No	No	427
CNS Cancer	SF-539	No	No	347
CNS Cancer	SNB-75	No	No	245
CNS Cancer	U251	No	No	468
Colon Cancer	COLO 205	Yes	No	407
Colon Cancer	HCC-2998	No	No	1413
Colon Cancer	HCT-116	Yes	Yes	457
Colon Cancer	HCT-15	Yes	Yes	490
Colon Cancer	HT29	No	Yes	363
Colon Cancer	KM12	No	No	468
Colon Cancer	SW-620	No	No	617
Leukemia	CCRF-CEM	Yes	No	380
Leukemia	HL-60(TB)	Yes	No	407
Leukemia	K-562	No	No	513
Leukemia	MOLT-4	Yes	No	912
Leukemia	SR	No	No	398
Melanoma	LOX IMVI	No	Yes	851
Melanoma	M14	No	Yes	347
Melanoma	MALME-3M	No	Yes	316
Melanoma	MDA-MB-435	No	Yes	195
Melanoma	SK-MEL-2	Yes	No	589
Melanoma	SK-MEL-28	No	Yes	1585
Melanoma	SK-MEL-5	No	Yes	389
Melanoma	UACC-257	No	Yes	407
Melanoma	UACC-62	No	Yes	501

NSC Lung Cancer	A549/ATCC	Yes	No	501
NSC Lung Cancer	EKVX	No	No	501
NSC Lung Cancer	HOP-62	Yes	No	589
NSC Lung Cancer	NCI-H226	No	No	1778
NSC Lung Cancer	NCI-H23	Yes	No	525
NSC Lung Cancer	NCI-H322M	No	No	525
NSC Lung Cancer	NCI-H460	Yes	No	363
Ovarian Cancer	IGROV1	No	No	447
Ovarian Cancer	NCI/ADR-RES	No	No	437
Ovarian Cancer	OVCAR-3	No	No	251
Ovarian Cancer	OVCAR-4	No	No	575
Ovarian Cancer	OVCAR-5	Yes	No	1549
Ovarian Cancer	OVCAR-8	No	No	479
Ovarian Cancer	SK-OV-3	No	No	562
Prostate Cancer	DU-145	No	No	457
Prostate Cancer	PC-3	No	No	282
Renal Cancer	786-0	No	No	490
Renal Cancer	A498	No	No	468
Renal Cancer	ACHN	No	No	851
Renal Cancer	CAKI-1	No	No	417
Renal Cancer	RXF 393	No	No	166
Renal Cancer	SN12C	No	No	912
Renal Cancer	TK-10	No	No	692
Renal Cancer	UO-31	No	No	513